Biogeochemistry
https://doi.org/10.1007/s10533-021-00794-8

The impacts of historical land-use on phosphorus movement in the Calhoun Critical Zone Observatory in the southeastern US Piedmont

Maryam Foroughi · John M. Mallard · Donald R. Nelson · Lori A. Sutter · Daniel Markewitz

Received: 5 September 2020 / Accepted: 7 April 2021

Abstract Human actions through land-use can alter soil phosphorus (P) distribution over time and space as vegetation is altered and added fertilizer P is translocated downslopes by runoff and erosion, or through the soil profile by leaching. In the southeastern US Piedmont, a more than 100-year period of human land-use of forest clearing and farming, which included P fertilization, caused severe surface erosion before reforestation. This history resulted in elevated surface soil P in farmed ridge tops, even after 70 years of reforestation, but little data exists on redistribution of this P downslope or down profile during these 70 years. We aimed to investigate the effect of different land-use histories on soil P losses over time. Combined with multiple years of current soils, soil solution, and stream water data from two small watersheds in the Calhoun Critical Zone Observatory (Calhoun CZO) in South Carolina, USA, we use the soil and water assessment tool (SWAT) to simulate a trajectory of seven different land-uses on P movement. Results indicated annual solution total P loss under 100% agriculture (3.7 kg ha^{-1} $year^{-1}$) was six times greater than under 100% forest while mixed forest and agriculture experienced about one-third the loss observed under agricultural land. Furthermore, the model predicted P leaching that ranged from 0.036 to 0.1 kg ha^{-1} $year^{-1}$ with the highest rates during early reforestation. These increased leaching rates could account for 7–20 kg ha^{-1} of vertical P movement through the soil profile over 200 years. This content of P leaching is consistent with observed differences in the content of extractable soil P in the 2 m of soil under farmed vs. never farmed locations. Simulation under high rainfall indicated wet periods or events could augment P mobilization and better approximated observed increases in soil extractable P content. These land-use change simulations indicate reforestation reduces surface runoff and erosion but increases vertical leaching and, despite soil P retention mechanisms, may move P deep into the soil profile.

Responsible Editor: Sharon A. Billings.

M. Foroughi (✉) · L. A. Sutter · D. Markewitz
Warnell School of Forestry and Natural Resources, University of Georgia, Athens, GA 30602-2152, USA
e-mail: foroughi.maryam64@gmail.com

L. A. Sutter
e-mail: lsutter@uga.edu

D. Markewitz
e-mail: dmarke@uga.edu

J. M. Mallard
Nicholas School of the Environment, Duke University, Durham, NC, USA
e-mail: john.mallard@duke.edu

D. R. Nelson
Department of Anthropology, University of Georgia, Athens, GA, USA
e-mail: dnelson@uga.edu

Published online: 22 April 2021

Keywords Soil phosphorus distribution · Calhoun Critical Zone Observatory · SWAT · Reforestation · Land-use

Introduction

Transformation of forest land to agricultural use and return to forest cover has left a legacy of impacts on forest soils (McLauchlan 2006; Richter and Markewitz 2001). Land-use and land management influence soil chemistry, soil erosion, and soil nutrient runoff to surface water (Grieve 2001; Johnes and Heathwaite 1997; Wang et al. 2010). Given a period of agricultural crop production and fertilization, these activities have particularly influenced soil phosphorus (P) and its landscape distribution (Aguiar et al. 2013; Alt et al. 2011; Foroughi 2019). A variety of attributes and actions impact P movement in watersheds such as inherent soil P concentration, P loading to the soil through fertilization or organic amendments, watershed land cover and clearing, tillage, topography, soil erodibility, and precipitation quantity and intensity (Dillon and Kirchner 1975; Osborne 1988; Sharpley et al. 1981; Sharpley and Smith 1990). For example, Sharpley et al. (1996) demonstrated how P loading that results in extractable soil P concentrations of > 200 mg kg^{-1} are excessive and likely to generate P runoff. Similarly, Elrashidi et al. (2005) exhibited increased water (1122 vs 939 m^3 ha^{-1}) and P (217 vs 190 g-P ha^{-1}) runoff in croplands compared to native grasslands. Finally, Sharpley (1985) revealed a clear link between increasing rainfall intensity (50–150 mm h^{-1}) and slope (2–20%) with the effective depth of surface soil generating P runoff (2–14 mm).

Two centuries of land-use history in the eastern US has followed a trajectory of forest to agriculture to afforestation that has extensively influenced soil properties (Compton and Boone 2000; Foster et al. 2003). The southeastern Piedmont of the US was particularly altered due to an extended era of cotton farming (Wear and Greis 2013). Land-use and land management changed in the Southeast from the 1700s to the 1800s with a transition from mature forest to cropland. Subsequently, the abandonment of agricultural land to afforestation occurred after the 1900s (Brender 1952; Cowell 1998). More than half of the eastern forest of the US was cleared and converted to farm, pasture, and industry in the nineteenth century (Williams 1992). By the twentieth century, however, the proportion of agricultural land in the southeastern Piedmont of the US began to decline (Hart 1980). For example, coniferous and deciduous forests covered less than 19% of the Georgia Piedmont in the 1930s when agricultural land comprised 81% (Turner and Ruscher 1988). By 1980, agricultural land declined to 36% whereas the coniferous forest distribution increased to 41%. Recently, in 2016, forests covered more than 67% of Georgia and South Carolina (Vogt and Smith 2017).

Well-known soil legacies of this history of land clearing and farming in the southeastern US include excessive surface soil erosion (Hall 1949; Ireland et al. 1939; Trimble 2008) and P enrichment (Richter et al. 2006; Richter and Markewitz 2001). Nearly 17 cm of surface soil is estimated to have eroded from hillslopes in the Southeast between 1750 and 1950 (Trimble 2008). During this period, there was increasing P fertilization in upland locations (Ruffin 1852) and surface soil extractable P is still elevated due to these practices (Richter and Markewitz 2001). For example, in the Piedmont of South Carolina in 2017, when comparing hardwood forest soils that were never farmed to forest soil under 70-year-old afforesting crop fields, extractable P was still 50–100% greater (4 to 6 μg-P g-soil^{-1} in surface soil or 2 to 4 μg-P g-soil^{-1} in subsoil) than in the never farmed hardwood forest; this difference was evident through 2 m of soil (Foroughi 2019). Phosphorus enrichment in the topsoil horizons of agricultural land can lead to P leaching loss and P movement with soil erosion (Hurtt et al. 2006), and a strong correlation between agricultural land-use and P movement into streams has been demonstrated (Nielsen et al. 2012). On the other hand, in the South Carolina location noted above, after 70 years of afforestation total soil solution P was lower in abandoned sites compared to the never farmed reference and 1st order streams in afforested watersheds typically had < 1 μmol P L^{-1} (Foroughi 2019). The transition from high P fluxes during agriculture to low P fluxes under afforestation while soil P remains elevated is difficult to resolve mechanistically given a lack of long-term measurements.

Recent reviews of agricultural legacies on soil and solution P (Deng et al. 2017; Goyette et al. 2018; MacDonald et al. 2012) have all addressed the dichotomy observed above of the potential for high P loss during agricultural use due to surface runoff but with long-term persistence of soil P enrichment. This elevated soil P suggests P sorption by clay, and P bonding with Al and Fe. MacDonald et al. (2012), for example, using a meta-analysis of 94 studies, demonstrated a clear increase in extractable and total soil P in abandoned agricultural land compared to reference sites with no farming history (similar to results documented above for South Carolina). On the other hand, this research also indicated that abandoned areas, depending on current land-use, had lower soil total P than current agricultural areas. This suggests that although soil total P is enriched after abandonment some soil P continues to be lost and land-use might influence the rate of loss. Deng et al. (2017) specifically looked at abandoned agricultural areas in 220 independent sampling sites that had been afforesting. In these areas, the soil total P content had an overall decline (12% on average) with afforestation but no measurable change in extractable P concentrations ($\sim$ 27 µg-P g-soil^{-1}), highlighting a continued loss of P but also a buffering of the extractable P pool (Richter et al. 2006; Schmidt et al. 1997). These findings also highlighted that soil total P declined most in afforesting tropical sites with high rainfall suggesting that rainfall inputs may play an important role in soil total P loss. Finally, Goyette et al. (2018) reconstructed 110 years of P fluxes in 23 watersheds and concluded that the time to eliminate legacy P in runoff might range from 100 to 2000 years. They also suggest this variance is a function of rainfall and land-use.

In the southeastern US Piedmont today, we found extractable P-enriched soils through 2 m but also limited soil solution P and low first-order stream water P concentrations (Foroughi 2019). The quantity of P lost to streams or leached through the soil profile when these lands were transforming from active agriculture to afforestation over 200 years is not well known. Modeling P solution fluxes through soils and to streams during these land-use changes may help us to understand these land-use dynamics (Veldkamp and Verburg 2004). Previous modeling studies have investigated the impact of land-use and climate changes on runoff and P flows (Jiang et al. 2018; Mehdi et al. 2015; Wilson and Weng 2011). For example, Mehdi et al. (2015) highlighted how combining land-use and climate change scenarios could increase the loss of solution total P by eightfold compared to climate change scenarios alone. Similarly, Wilson and Weng (2011) tested the effect of future urban land-use and climate changes on water quality in the Chicago metropolitan area. Their findings showed that solution total P concentration should decline in watershed streams by 2–18% as a result of a reduction in agricultural land.

Our objectives for this modeling study were to: (1) assess the legacy effect of land-use changes on the surface and subsurface movement of P and (2) determine the impact of precipitation inputs on surface and subsurface P movement under these different land-use scenarios. Based on our present-day soil and solution P data, we hypothesized that under cultivation and P fertilization our model would estimate P solution fluxes in surface water due to runoff and soil erosion that are an order of magnitude higher than today (e.g., $>$ 10 kg-P ha^{-1} year^{-1}). Thereafter, loss of P would decrease with agricultural land abandonment and afforestation. During this period, however, we hypothesized that as surface runoff declined that part of the applied fertilizer P would be leached through the soil profile. We also expected, based on previous research, that solution total P fluxes would increase when the precipitation rate was increased but that this influence would be greater when the land was still under agricultural use due to more soil and sediment runoff to the stream. Overall, we employed model simulations to test our hypothesized trajectories of soil and solution P dynamics during 200-years of land-use conversion in the southeastern US Piedmont.

Methods

Study site

Our study watersheds, W4 of 8.75 ha and W3 of 10.3 ha, are situated in the Calhoun CZO within the Sumter National Forest (34° 7′ 55.36″ N, 82°18′ 36.17″ W) in Union County, SC (Fig. 1). Elevation ranges from 125 to 172 m and nearly 85% of the watershed slope is 0–30% (Fig. 2). The average temperature and annual precipitation of this region between 2011 and 2018 were 17°C and 1185 mm, respectively (Clinton, SC; https://www.ncdc.noaa.gov/cdo-web/). According to the National Land Cover Database (NLCD), approximately, 93% of

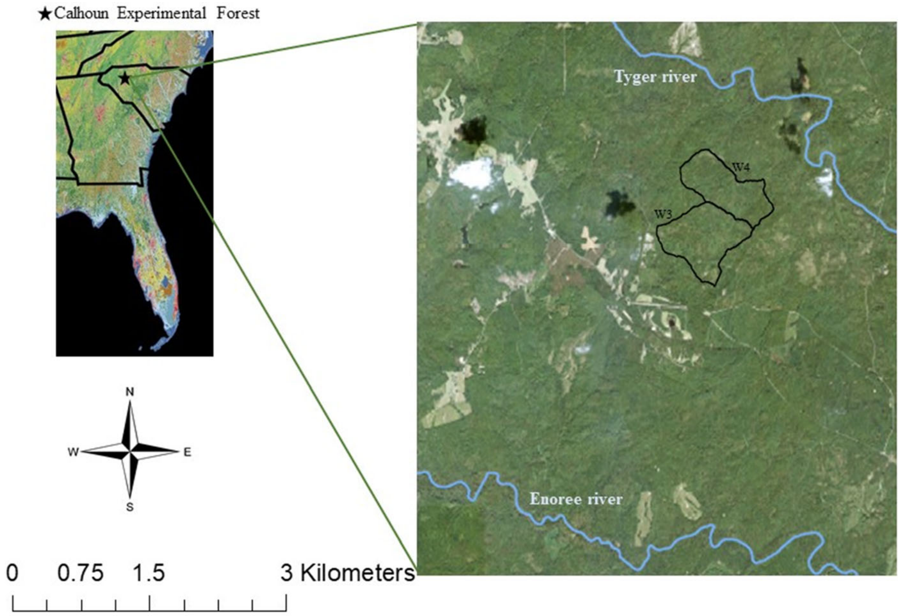

Fig. 1 Study location in the Calhoun Critical Zone Observatory, South Carolina, USA. W4: Calibration watershed, W3: Validation watershed

these watersheds are covered by forest (deciduous and pine) and 7% by grasses (Fig. 2).

Land-use history data and scenarios

Land-use history data were derived from US Forest Service (USFS) archives that contained legal descriptions, maps, deed abstracts, and other records about the land acquisition by the US Forest Service. At the time of purchase, the USFS recreated deed chains for each property, going back to the original land grant, whenever possible. When land transactions occurred, whether, through sale, inheritance, partitioning, or other mechanisms, surveyors mapped the property using the metes and bounds system (Pettus 1995). The metes and bounds surveys fixed property boundaries based on landscape features (including trees, rivers, and later, as trees became scarcer, stakes and rocks) and compass bearings. For each property, the landscape features were recorded for each historical transaction and later aggregated into hardwood, pine, open, and water categories (Fig. 3). The figure incorporates data recorded from all the properties in the research site. The category counts for each decade represent the sum of transaction records for the previous 10 years (e.g., 1850 includes data from 1841 to 1850). The Calhoun CZO was covered with mixed hardwood forest before 1800, then the upland forest was converted to agricultural land (Gray and Thompson 1933; Metz 1958; Ruffin 1852). Furthermore, farmers applied P fertilizer and lime to the land after intensive deforestation (Sheridan 1979; Taylor 1953). Most of the agricultural lands were abandoned and then converted to regrowing forest or pasture in the early twentieth century (Metz 1958; Richter and Markewitz 2001). Land-use history data for the Calhoun CZO revealed that hardwood forest declined from $\sim$ 65% to < 20% between 1790 and 1910 while open land (i.e., agricultural land) increased to $\sim$ 80% in 1910. Thereafter, between 1910 and 1940 open land declined to $\sim$ 50% while hardwood and pine forest re-developed slowly to cover $\sim$ 25 and 10% of the landscape, respectively (Fig. 3).

Based on these specific records for the Calhoun CZO and other historical accounts for the region, scenarios for model simulation were developed. Six land-use scenarios were created (Fig. 4) to approximate the forest to cropland to afforestation trajectory. The starting watershed condition is covered with mature deciduous forest (i.e., deciduous forest). Thereafter, flatter, upland areas that were likely cleared first are converted to agricultural land for a

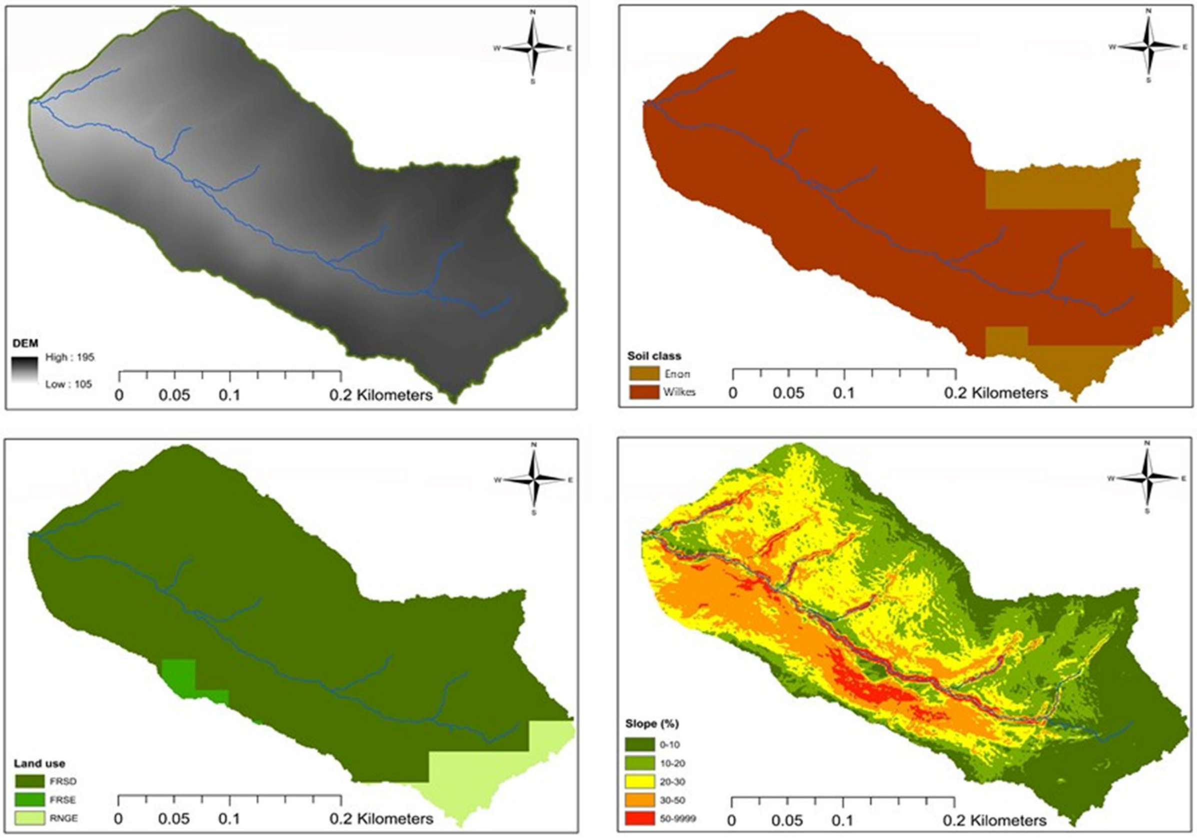

Fig. 2 ArcSWAT input data for calibration watershed W4 in the Calhoun Critical Zone Observatory, South Carolina, USA. *DEM* Digital elevation map, *FRSD* deciduous forest, *FRSE* evergreen forest, *RNGE* grasslands

mixed land-use watershed (agriculture-deciduous forest). The next step assumes less desirable lands (i.e., steeper) were cleared and brought into agriculture such that 100% of the watershed area is converted to agricultural land (i.e., agriculture). As economic and environmental conditions changed it is presumed some of the less desirable lands were abandoned and pine forests started to develop on these hillslopes (pine forest-agriculture). Eventually, agriculture in the uplands is abandoned and the whole watershed area is covered with pine forest (i.e. pine forest). Finally, the most recent land-use that approximates current conditions is a mixture with the pine trees persisting in the flatter upland and hillslopes reverting to a deciduous forest (mixed forest) (Fig. 4). The current NLCD map contains around 7% grassland, which is inconsistent with observations so was not considered in the simulation scenarios.

Reported rates of historical fertilization indicate that farmers normally applied 224–336 kg ha^{-1} fertilizer with 11-20-13 (N-P-K) or 560–673 kg ha^{-1} 4-10-6 fertilizer (Sheridan 1979; Taylor 1953). Based on these reports, the agricultural land area in each scenario received annual inputs of 250 kg ha^{-1} fertilizer application of N-P-K (11-20-13). Initial extractable soil P was increased to 20 μg g^{-1} after agricultural abandonment based on reported values for agricultural land after afforestation at the Calhoun CZO (Richter et al. 2006). Similarly, soil extractable P was set to 5 μg g^{-1} for the current land-use scenario based on measurements from the watersheds in 2017 (Foroughi 2019). Each scenario is simulated for 10 years and the results are reported as an average over the 10 years. Initial extractable soil P was set to the measured reference conditions (2 μg g^{-1}). All these land-use scenarios were simulated with either normal precipitation, an annual input of 1169 mm, or high precipitation, 2688 mm, which is consistent with the highest rainfalls recorded between 1979 and 2014 (https://www.ncdc.noaa.gov/cdo-web/).

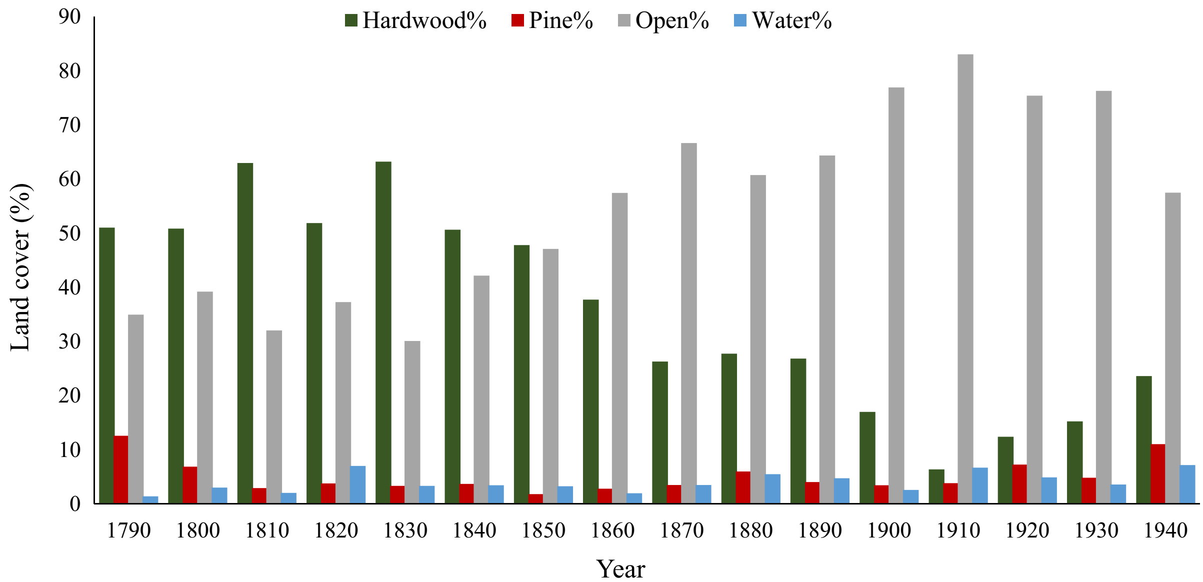

Fig. 3 Land cover changes at the Calhoun Critical Zone Observatory in the Sumter National Forest, South Carolina, USA from 1790 to 1940

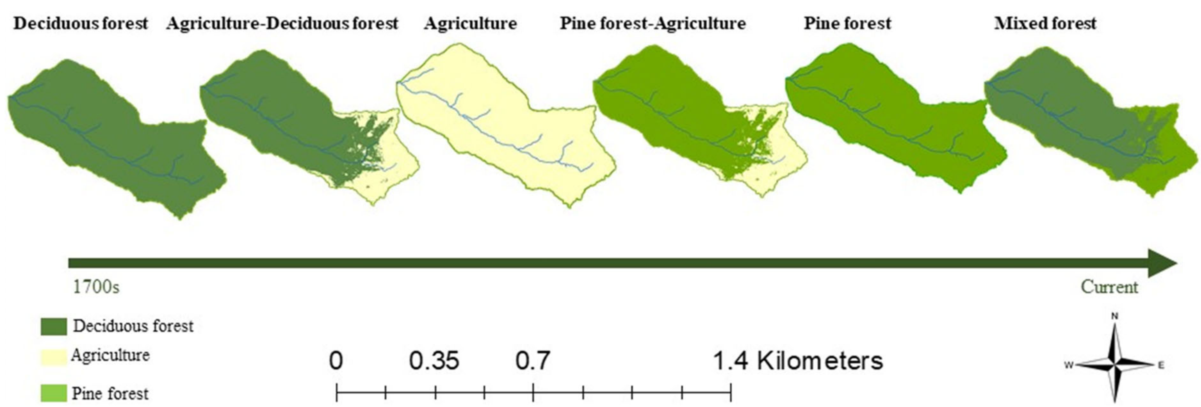

Fig. 4 Land-use scenarios for the calibration watershed W4 in the Calhoun Critical Zone Observatory, South Carolina, USA

SWAT model description

The Soil and Water Assessment Tool (SWAT) was implemented to determine the influence of land management activity on streamflow (discharge), P loss into runoff, and P leaching through soil horizons (Arnold et al. 1993, 1998). We chose the SWAT model because of its broad application in addressing questions related to land management changes (Arabi et al. 2006; Rocha et al. 2015; Ullrich and Volk 2009). The SWAT model predicts the effect of different land-use and land management on the quantity and quality of water and soil over multiple years (Arnold et al. 1998; Neitsch et al. 2011). SWAT employs a daily time step which can subsequently be aggregated to report monthly output (Wilson and Weng 2011). Based on a digital elevation model (DEM), the study watershed is divided into sub-watersheds that contribute to a stream. Each sub-watershed is further divided into multiple hydrological response units (HRU), each comprising the watershed area with unique soil type and land-use. Surface runoff, evapotranspiration (ET), subsurface lateral flow, canopy interception, and other components of the water balance are calculated for each HRU individually and summed across sub-watersheds (Gassman et al. 2007). SWAT uses a

Table 1 Streamflow and phosphorus parameters, fitted values, and P-values from calibration of the model in SWAT-CUP (Soil and Water Assessment Tool Calibration and Uncertainty Program)

Parameter	Description	Fitted value	P-value
Flow parameters			
r__CN2.mgt	Runoff curve number II	− 0.095	$1.34e^{-66}$
v__ALPHA_BF.gw	Exponential decay factor for groundwater flow to the stream (1/day)	0.598	0.579
v__GW_DELAY.gw	Ground water delay time (days)	70.48	0.265
v__GWQMN.gw	Threshold depth of water in the shallow aquifer (mm)	0.075	0.714
v__GW_REVAP.gw	Groundwater re-evaporation coefficient	0.175	0.220
v__TRNSRCH.bsn	Fraction of transmission losses from main channel (m^3/s)	0.487	$2.74e^{-27}$
v__CH_K2.rte	Effective hydraulic conductivity of the alluvium in the main channel (mm/hr)	11.30	$1.34e^{-66}$
v__CH_K1.sub	Effective hydraulic conductivity in tributary channel alluvium (mm/hr)	197.5	0.638
v__CH_N2.rte	Manning's roughness coefficient of the main channel	0.157	0.024
v__SURLAG.bsn	Surface runoff lag coefficient	4.144	0.546
r__SOL_K().sol	Saturated hydraulic conductivity (mm/hour)	0.223	0.252
r__SOL_AWC().sol	Available water capacity of the soil horizon (mm H_2O/mm soil)	1.140	0.243
r__SOL_BD().sol	Moist bulk density (g/cm^3)	− 0.090	1.884
v__ESCO.bsn	Soil evaporation compensation factor	0.498	0.831
v__EPCO.bsn	Plant uptake compensation factor	0.170	0.570
Phosphours parameters			
v__PPERCO.bsn	Phosphorus percolation coefficient	13.05	0.107
v__PSP.bsn	Phosphorus sorption coefficient	0.824	0.789
v__ERORGP.hru	Organic P enrichment ratio	4.791	$1.56e^{-15}$
v__RSDCO.bsn	Residue decomposition coefficient	0.006	0.937
v__PHOSKD.bsn	Phosphorus soil partitioning coefficient	164.1	$2.65e^{-07}$

modified curve number approach (USDA-NRCS 2004) to calculate surface runoff and the Penman–Monteith method to calculate ET (Monteith 1965). Percolation into subsurface soil horizons is calculated as a function of soil water volume and saturated hydraulic conductivity, while the lateral subsurface flow is modeled using a kinematic wave approximation; upwelling and return flow are driven by saturation in the shallow aquifer or deeper soil horizon components (Arnold et al. 1998).

Soil P in the SWAT model included inorganic and organic pools, with each of these pools divided into three pools: solution, active, and stable for the inorganic pool and fresh, active, and stable for the organic pool. Interactions between these pools are controlled by their concentrations, physical characteristics of the soil (e.g., temperature), relevant rate constants, and stoichiometric relationships with modeled C and N. Phosphorus loss into the stream is composed of both dissolved inorganic P in solution and total P that includes P adsorbed to eroded sediment. P leached into the soil profile was calculated as a function of soil water infiltration and the vertical P concentration that accounts for plant uptake of labile P (Chaubey et al. 2006). Though SWAT generates dozens of outputs, for this study, we focused on outputs for discharge, P loss into the stream, and P leached into the soil profile.

SWAT input data

The ArcSWAT 2012 interface was used to build this model using a DEM with 1 × 1 m resolution, a land-use map obtained from the National Land Cover Database (http://www.mrlc.gov), and the Soil Survey Geographic Database (SSURGO) extracted from the

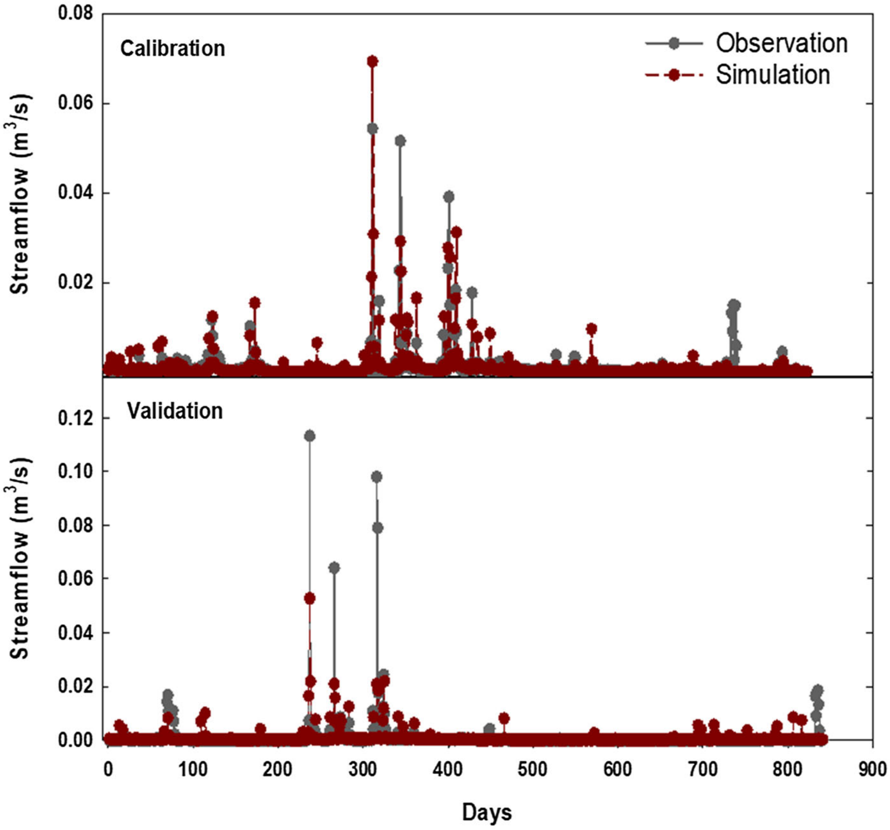

Fig. 5 The observed and simulated data for daily streamflow in the calibration and validation watersheds in the Calhoun Critical Zone Observatory, South Carolina, USA

web soil survey (https://websoilsurvey.sc.egov.usda.gov/). Climate data were gathered from the National Oceanic and Atmospheric Administration (https://www.ncdc.noaa.gov/cdo-web/) using the nearby Clinton, SC station including maximum and minimum temperature, and precipitation. In addition, onsite precipitation data for 2015 and 2016 were available and utilized [(Mallard 2017); unpublished data]. According to the soil map, most parts of the watersheds (87.8%) are loamy, mixed, active, thermic, shallow Typic Hapludalfs with a small portion (12.2%) of the upland as fine, mixed, active, thermic Ultic Hapludalfs (12.2%). Field observation and soil analysis classify these soils as Kanhapludults and Hapludults, which are more acidic and base poor but texturally similar. For model purposes, we used the available map designations. The soil horizons (and range in thickness) are generally A (≤ 7.6 cm), E (7.6–20 cm), Bt or Be (15–53 cm), Bt1 (25–84 cm), and Bt2 (33–122 cm).

Model calibration and validation

Stream discharge was consistently measured in watersheds W3 and W4 during 2015–2017 and these data were used to calibrate and validate the model for streamflow [(Mallard 2018); unpublished data]. Furthermore, monthly stream samples were collected in these same watersheds to measure P concentration through 2014–2017. SWAT was calibrated using W4 for daily and monthly streamflow, monthly solution total P, and monthly solution inorganic P with the SWAT Calibration and Uncertainty Program (SWAT-CUP) version 5.2 using the SUFI2 (sequential uncertainty fitting) version 2 (Abbaspour 2012; Abbaspour et al. 2007). The daily and monthly streamflow were initially calibrated with 15 parameters, then the P concentration parameters were calibrated. According to the calibration process, the sensitive parameters for streamflow and P were adjusted in SWAT (Table 1). The validation model was performed for daily and

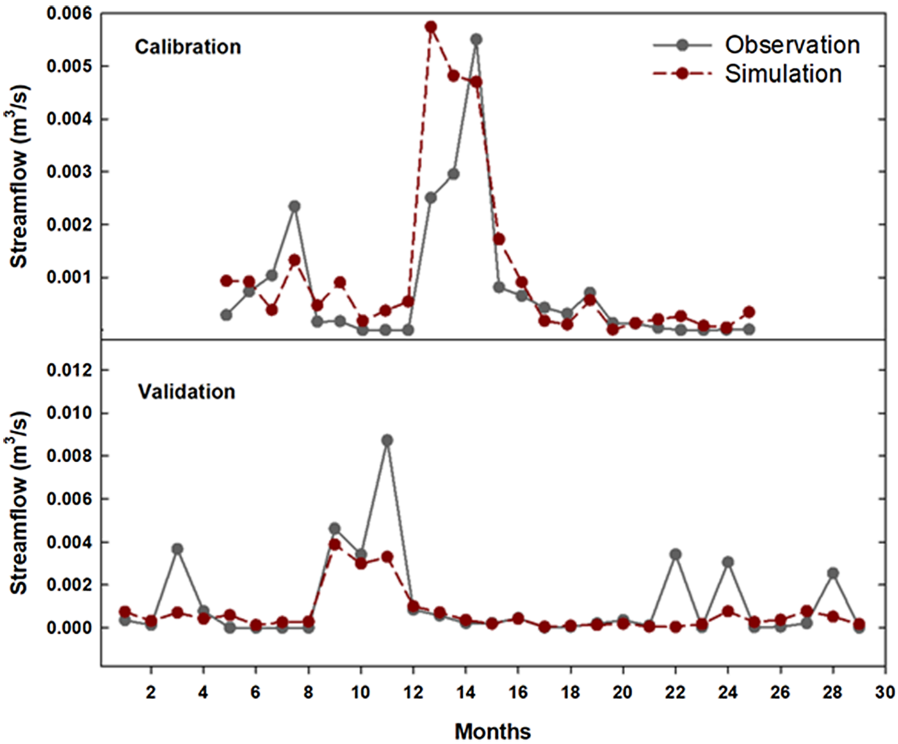

Fig. 6 The observed and simulated data of monthly streamflow in the calibration and validation watersheds in the Calhoun Critical Zone Observatory, South Carolina, USA

Table 2 Primary objective functions to evaluate the correspondence between predicted vs observed values in calibration (W4) and validation (W3) watersheds of the Calhoun Critical Zone Observatory, South Carolina, USA

Items[a]	Time	Criteria[b]	Calibration	Validation
Streamflow (m^3/s)	Daily	RMSE	0.003	0.005
		NSE	0.620	0.590
		r^2	0.620	0.480
Streamflow (m^3/s)	Monthly	RMSE	0.001	0.001
		NSE	0.720	0.550
		r^2	0.750	0.590
Solution total P (kg/ha)	Monthly	RMSE	1.420	0.970
		NSE	0.390	0.340
		r^2	0.520	0.820
Solution inorganic P (kg/ha)	Monthly	RMSE	0.040	0.020
		NSE	0.460	0.310
		r^2	0.500	0.830

Data for streamflow and P loss in calibration and validation are from 2014 to 2017. r^2 and NSE equal to 1 and RMSE to zero are best

[a]*P* phosphorus

[b]*NSE* Nash-Sutcliff Efficiency, r^2 Coefficient of determination, *RMSE* Root mean square error

monthly discharge and monthly P for W3 with the same condition of soil type, land cover, hydrology, and slope (Fig. 2). The coefficient of determination (r^2), Root Mean Square Error (RMSE), and Nash–Sutcliffe Efficiency (NSE) were used as the primary objective functions for calibration and validation. The NSE is a standardized measurement demonstrating how well the predicted and observed data fit the 1:1 line with values nearer to 1 suggesting a model with more predictive skill (Nash and Sutcliffe 1970).

Result and discussion

Calibration and validation

The calibration between observed and simulated discharge in daily and monthly time steps were generally highly correlated (r = 0.70–0.86) in Figs. 5 and 6, respectively. Occasionally, peak observed and predicted discharge values were not well correlated, which may relate to the lack of onsite rainfall data. The r^2 and NSE between daily observed and simulated streamflow were $\geq$ 0.48 for both W4 and W3 (Table 2). Similarly, the NSE of monthly calibration and validation for streamflow were 0.72 and 0.55, respectively (Table 2). Observed and simulated solution total P and inorganic P were also generally well aligned (Fig. 7). The monthly calibration had NSE with a range of 0.39 for solution total P and 0.46 for solution inorganic P. For the validation, the NSE were 0.34 and 0.31 for the monthly solution total P and inorganic P, respectively (Table 2).

Streamflow

Using the calibrated model based on the current conditions described above we simulated the different land-use change scenarios for discharge. The model simulation starting with deciduous forest found 38% (453 mm) of annual precipitation as runoff. As uplands were initially cleared (agriculture-deciduous forest) runoff increased to 41% percent (482 mm). After 100% of the watershed was converted to agriculture, runoff reached 563 mm or 48% as runoff (Fig. 8). During initial agricultural abandonment under pine forest-agriculture with secondary pine forests on the hillslopes, runoff declined to 37%. Finally, as land-use reverted to fully forested conditions under pine forest and mixed forest runoff was 36% (418–420 mm). Thus, the simulation of different land-use scenarios with SWAT indicated that streamflow through the study watershed increased as a percent of input by 3 to 10% when 20 to 100% of the area was converted to agricultural use (Fig. 8). This finding is well-supported by previous research, with decreasing forest or increasing agricultural cover in watersheds consistently corresponding to increases in streamflow (Brown et al. 2005; Hornbeck et al. 1993).

Fig. 7 The observed and simulated data of solution total phosphorus and inorganic phosphorus for the calibration and validation watershed in the Calhoun Critical Zone Observatory, South Carolina, USA ▶

Deforestation results in less soil organic matter in and on the topsoil thus decreases the infiltration rate. Evapotranspiration is also lower from agricultural land compared with forest land. Both these processes lead to a greater proportion of precipitation moving to surface runoff. In the current model, runoff increased annually by 16–25% when 100% of the watershed was agricultural land in comparison with forest-agriculture and 100% forest land-use, a result within the range of previous studies. For example, in a multi-site study including sites in New Hampshire, West Virginia, and North Carolina, Jones and Post (2004) found deforestation increased runoff around 18% (from 4 to 21%) depending on the watershed.

Reforestation of previously agricultural land resulted in a decrease in runoff, coincident with an increase in the infiltration rate. This infiltration rate increase likely results from a decrease in surface soil bulk density and an increase in porosities built up by root activity and higher surface organic matter. In comparison with agricultural land, forest land has improved soil structure (Mapa 1995). A review of 167 reforestation studies globally found 80% reported declines in water yield (Filoso et al. 2017). In the southeastern Piedmont, an increase of reforestation from 1919 to 1967 ranging from 10 to 28% of the area caused a decrease of 4–21% in surface runoff (Trimble et al. 1987). Interestingly, our simulated streamflow water yields remain slightly below their pre-agricultural levels as coniferous and deciduous trees replace agricultural land (Fig. 8). Other studies have observed higher water use among young trees relative to older ones (Hornbeck et al. 1993; Swank et al. 2001), and

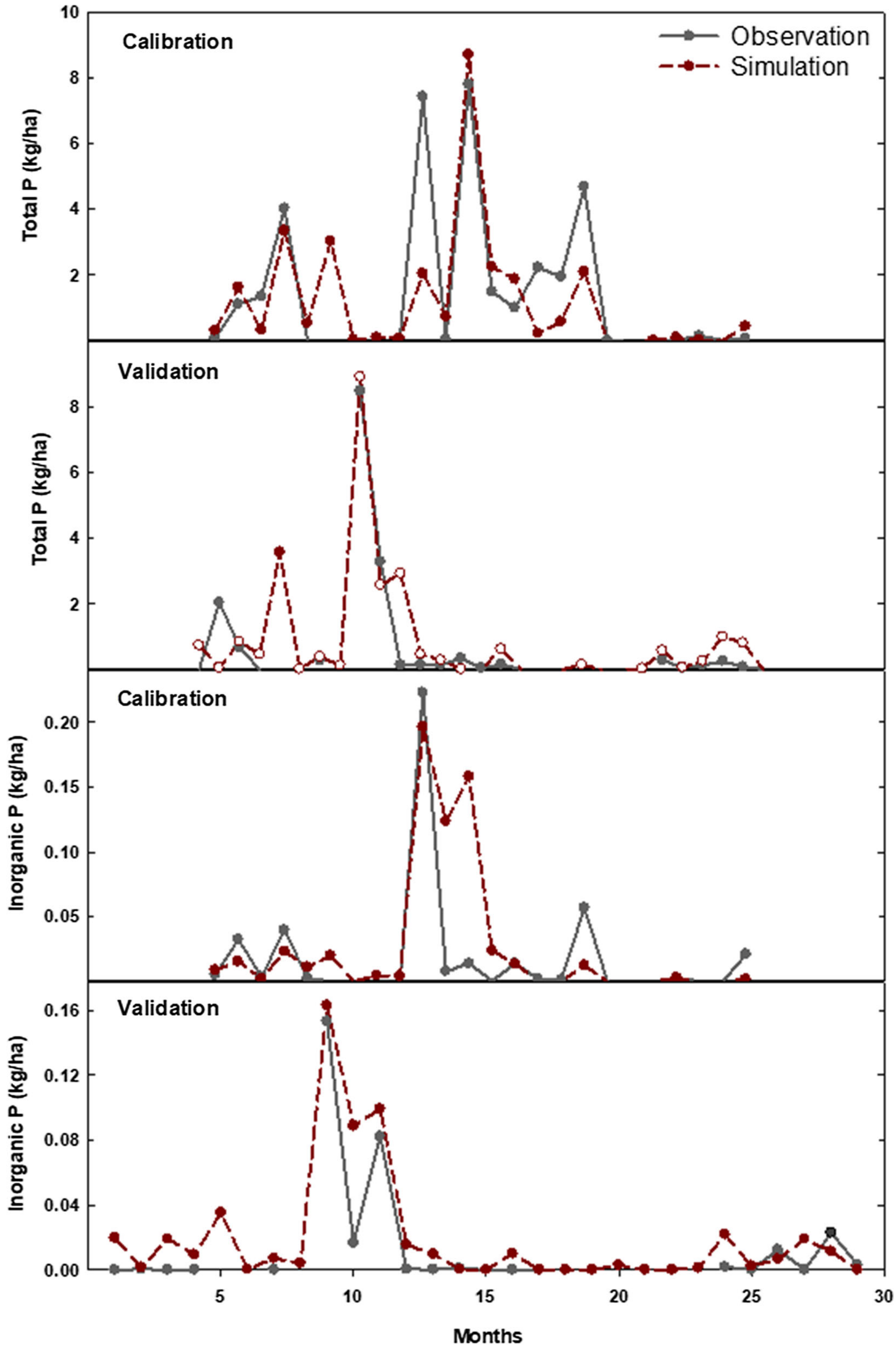
Calibration
Observation
Simulation
Total P (kg/ha)
Validation
Total P (kg/ha)
Calibration
Inorganic P (kg/ha)
Validation
Inorganic P (kg/ha)
Months

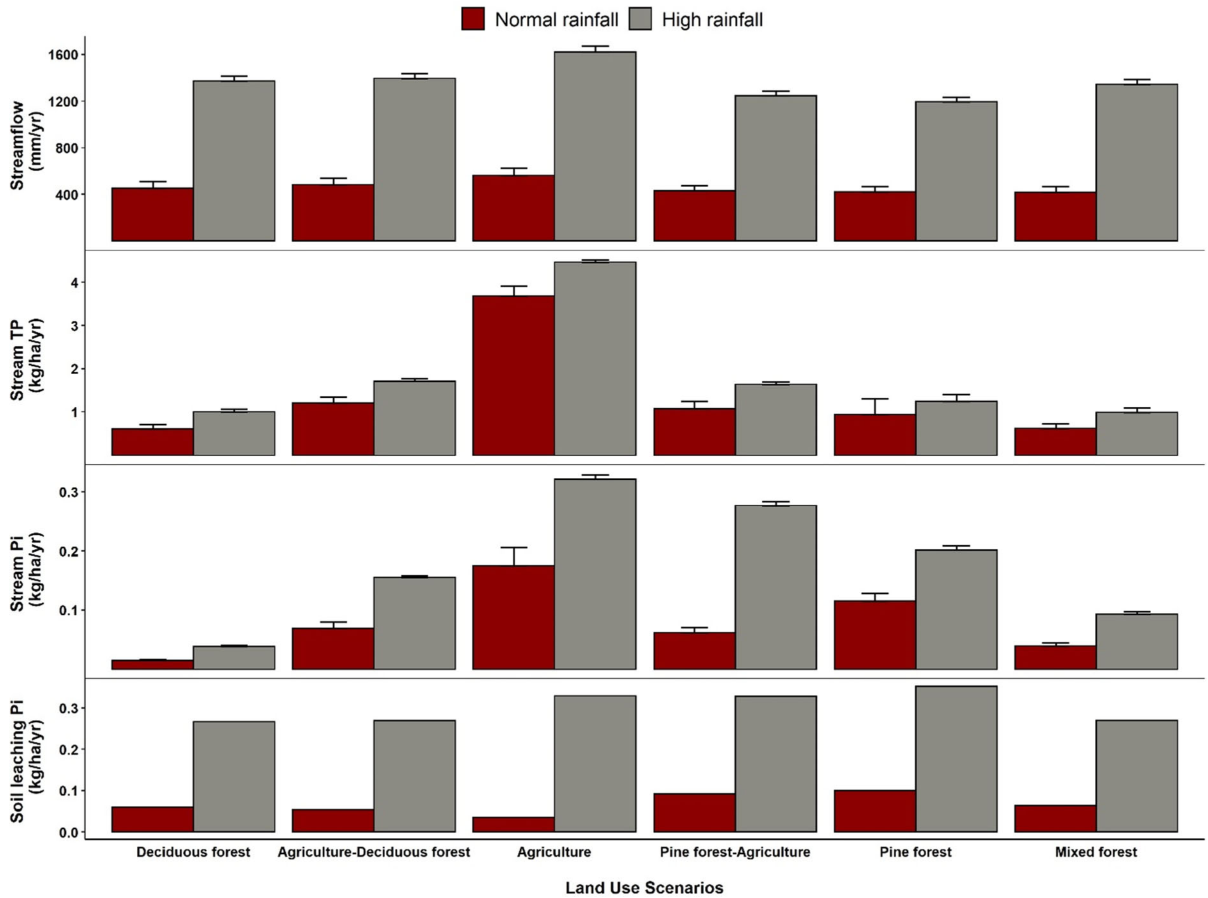

Fig. 8 Simulated streamflow, solution total phosphorus (stream TP) and solution inorganic phosphorus (stream Pi) in streams, and solution inorganic phosphorus (soil leaching Pi) to the subsoil layer for different land-use and climate scenarios. Streamflow, stream TP, and stream Pi are an average (1SD) of annual means output for 10-year simulation under each land-use. Leaching rates are output as a 10-year average mean rate

our simulation suggests legacies of land-use change may persist past their apparent recovery.

The interaction of land-use changes and precipitation magnitude on stream discharge varied across the land-use scenarios. For the high rainfall simulations using the same land-use scenarios, the amount of precipitation was increased twofold (1169 to 2688 cm). With higher precipitation, the model predicted a runoff increase from 453 to 1371 mm per year under deciduous forest and from 562 to 1620 mm with agricultural land cover (Fig. 8). Relative to rainfall input, percentage change of runoff output increased 8.5–11.5% under forest and > 12% under agricultural land. This difference in sensitivity to increased precipitation can likely be attributed to both the modified physical characteristics of agricultural soils (Zimmerman et al. 2006) and elevated evapotranspiration (primarily transpiration) of forests (Stoy et al. 2006). The greatest difference in percent runoff was between agricultural land with high precipitation compared with forest land-use under average precipitation (Fig. 8). Other studies have demonstrated the clear effects of both land-use and precipitation changes on streamflow. In a watershed in Ontario, Canada El-Khoury et al. (2015) observed an 8.5–11.2% increase in streamflow due to precipitation increases and a 1.2–2.6% increase in streamflow due to land-use changes. In another model simulation conducted in Brazil, watershed stream discharge decreased 39–57% due to a 20–32% reduction of precipitation (Von Randow et al. 2019). These studies along with our study highlight the complexity of these concurrent drivers of change in streamflow, where we find higher but less relatively variable streamflow in agricultural land under extreme conditions (Fig. 8). Our simulation indicates that changes in both precipitation inputs and land-use can result in non-linear streamflow responses. Overall, the model prediction of increasing streamflow when mature hardwood forests are cleared and converted to agriculture followed by streamflow reduction with afforestation after abandonment of agriculture is well-supported by previous research and provides a solid basis for considering historic P movement.

Patterns of P loss

Total P loss increased by $\sim$ sixfold from 0.6 to 3.7 kg ha^{-1} year^{-1} when 100% mature deciduous forest was converted to 100% agricultural land, which included the application of P fertilizer (Fig. 8). This increase in P runoff from fully forested (deciduous forest) to fully agriculture followed a rising and falling pattern with land-use conversion and recovery. Similar to the discharge patterns, mixed land-uses had an intermediate level of P runoff compared to deciduous forest and agricultural land. When upland portions of the watershed were agriculture, but the rest was covered with forest (agriculture-deciduous forest and pine forest-agriculture), the solution total P loss ranged from 1 to 1.2 kg ha^{-1} year^{-1} (an increase of 50%). As land returned to fully forested (pine forest and mixed forest) loss of solution total P ranged from 0.6 to 0.9 kg ha^{-1} year^{-1}.

Based on these P outflows and according to land-use histories for the southern US Piedmont, $\sim$ 560 kg ha^{-1} P could have been lost over 150 years of cultivation. In comparison to a similar period of forest (deciduous or mixed forest) cover, just 90 kg ha^{-1} P would have exited. The greater loss of P to stream water in agricultural land results largely from annual applications of P fertilizer but harvesting activities, the loss of deep tree roots in forests, and the accelerated erosion of soil P with sediments also contribute. Multiple prior studies have quantified the role of current agricultural activities in causing soil erosion and transport of soil nutrients to streams (Carpenter et al. 1998; Sharpley and Withers 1994). Agricultural activities such as tillage disturb soil aggregates, decrease soil organic matter, reduce hydraulic conductivity, and interrupt earthworm and macroinvertebrate activities, all causing a decline in infiltration and an increase in erosion (Lindstrom et al. 1994). In contrast, reforestation of prior agricultural land can restore these attributes and decrease losses of different forms of P in surface runoff by up to 30% (Wang et al. 2012). Recent research in the Calhoun CZO watersheds measured limited P ($\sim$ 1 µmol L^{-1}) in surface water after 70 years of forest regrowth, although extractable P in soils is still elevated due to former agricultural fertilization. These data demonstrate the effect of reforestation on limiting P movement in runoff relative to crop land (Foroughi 2019).

The accumulation of soil P when P fertilizer is applied to agricultural land increases the potential for P movement from soil to stream (Elrashidi et al. 2005; Sharpley et al. 1996). Historical research about the southeastern Piedmont reported that farmers added animal manure to the land until about 1870–1873 when superphosphate fertilizer production was begun in Charleston, SC (Sheridan 1979). We used this information to simulate 250 kg ha^{-1} of 11-20-13 fertilizer application or 50 kg ha^{-1} of P. Given the various sources of P (manure and superphosphate) as well as uncertain formulations of superphosphate it is hard to estimate exactly how much P as fertilizers was added to our Calhoun CZO watershed over 150 years. If, however, we assumed sustained inputs of 50 kg ha^{-1} for 150 years the total input is 7500 kg ha^{-1}. Currently, measured total soil P through 2 m of soil with an agricultural history has $\sim$ 4000–6000 kg-P ha^{-1} but this is not greater than profiles measured in areas without previous agriculture (Foroughi 2019). As such, we might expect high rates of P loss when 100% of the simulation watershed was agricultural land with 50 kg ha^{-1} P fertilizer added to the surface soil. Under this model condition, however, only 3.7 kg ha^{-1} year^{-1} total P moved annually from soil to stream. In addition to stream export (3.7 kg ha^{-1} year^{-1}), plant P uptake may account for an additional $\sim$ 5–6 kg-P ha^{-1} year^{-1} of fertilizer inputs based on our model output, which still leaves 82% of P fertilization in soil mineral stocks. After 70-years of afforestation, current total soil P measurements do not account for any of this un-exported fertilizer P.

Given the limited P loss relative to inputs noted above, we combined land-use changes with precipitation conditions addressing whether periods of high rainfall (or specific high rainfall events such as hurricanes) may have a disproportionate effect on P loss. The response of solution total P loss to rainfall quantity (from 1169 to 2688 cm) was an increase from 0.6 to 1 kg-P ha^{-1} year^{-1} on average when the watershed was covered with mature hardwood forest (deciduous forest). Under higher rainfall, the solution total P loss increased by $\sim$ 1.5-fold (1.2 to 1.7 kg ha^{-1}) when uplands were initially cleared (agriculture-deciduous forest). The highest loss of solution total P occurred when the watershed was under agriculture with high rainfall (4.46 kg ha^{-1}). Thereafter, along the trajectory but still with higher rainfall, the solution total P loss to surface water increased from 1.0 to 1.6 kg ha^{-1} under agriculture-pine forest, 0.9 to 1.2 kg ha^{-1} under pine forest, and 0.6 to 1.0 kg ha^{-1} under mixed forest (Fig. 8).

In comparison to the solution total P loss, which includes organic and mineral bound P, solution inorganic P followed the same pattern as solution total P in runoff but comprised a small percentage of the total. The model predicted that solution inorganic P loss increased during forest clearing and conversion to agricultural land. Under deciduous forest, solution inorganic P loss was 0.02 kg ha^{-1} while the highest loss of solution inorganic P was 0.18 kg ha^{-1} when the entire watershed was under cultivation (Fig. 8). Again, solution inorganic P loss trended up and down with forest loss (agriculture-deciduous forest and agriculture) and recovery (pine forest-agriculture, pine forest, and mixed forest). Interestingly, solution inorganic P loss was higher under pine forest and mixed forest compared to deciduous forest, likely due to the historical application of P to agricultural land that increased extractable soil P concentration in model parameterizations. The content of solution inorganic P loss with the twofold increase in rainfall increased proportionally such that fluxes were 50–60% higher for all land-use scenarios. Increasing discharge in streams can dilute P concentrations but there is a strong correlation between streamflow volume and loss of P content (r = 0.47–0.82), which persisted for all the different land-use scenarios. Combining land-use and precipitation changes can cause a large increase in runoff and nutrient loss to streamflow (Tong et al. 2012). For example, in the Pheasant Branch watershed in Dane County, Wisconsin solution total P movement increased sixfold during a storm event compared to a period of average rainfall (7 kg ha^{-1} year^{-1}) when comparing pastureland and cultivated cropland (Huisman and Karthikeyan 2012). Similar storm event sampling in pastureland in the Georgia Piedmont showed an average of $\sim$ 0.1 kg total P movement in solution to streams per day that increased to 0.47 kg just after each storm (Byers et al. 2005).

In the Calhoun CZO, under the model conditions, changing land-use history under high rainfall could account for 735 kg ha^{-1} solution total P loss over 150 years when the watershed was agricultural land compared to 560 kg ha^{-1} solution total P loss under average conditions reported above. Thus, loss of P into stream and plant uptake could account for around 1600 kg ha^{-1} P over 150 years when the watershed was agricultural land. After agricultural abandonment and afforestation, 69 kg ha^{-1} P could be lost over 70 years under the high rainfall situation compared to $\sim$ 55 kg ha^{-1} P under average rainfall. The high rainfall simulation indicates that to the extent these years or events occurred they likely drove more P from the watershed, but the differences estimated here still do not account for 7500 kg ha^{-1} of fertilizer P inputs, suggesting lower P inputs or underestimated loss rates over this land-use trajectory.

Soil P leaching through the profile: land-use and precipitation changes

While land-use changes influence P movement with surface runoff, both through soil erosion and dissolved in surface runoff, a part of P movement is vertical as solution leaching through the soil profile. The model predicted that 0.06 kg ha^{-1} of solution inorganic P leached annually from the first soil horizon to the second soil horizon (below 7.5 cm) when land-use was mature hardwood forest (deciduous forest). Leaching of P into the soil declined to 0.05 kg ha^{-1} year^{-1} when the upland part of the watershed converted to agriculture (agriculture-deciduous forest). Phosphorus leaching was even slightly lower (0.036 kg ha^{-1} year^{-1}) when the entire watershed was converted to agricultural land. Leaching of solution inorganic P increased to 0.092 kg ha^{-1} year^{-1} with early afforestation in most of the watershed (pine forest-agriculture). Similarly, P leached around 0.1 kg ha^{-1} year^{-1} when the watershed converted to pine forest; however, it declined to 0.06 kg ha^{-1} year^{-1} after the watershed reforested to mixed forest (Fig. 8). A lower volume of surface runoff was predicted under forest land-uses due to greater surface infiltration compared with agricultural land. This greater infiltration resulted in increased vertical P leaching. P leaching is influenced by land cover, management activities, and the quantity of fertilizer application (Leinweber et al. 1999). Hydrologic flow rates are also a primary driver with P moving through the soil profile in proportion to flow (Akhtar et al. 2003). Finally, soil clays, including iron and aluminum oxides, can fix or adsorb P potentially slowing the down profile movement (Parfitt 1978).

Consistent with historical land-use changes in the Calhoun CZO, we previously found elevated extractable P in upper (0–30 cm) surface layers (Richter and Markewitz 2001) that we presume is a response to prior fertilization. More recently, when comparing soil through 2 m in lands known to have been farmed previously relative to reference sites, we found increases in soil extractable P throughout the profile (Foroughi 2019). We presume this is a result of vertical soil P leaching, although this is inconsistent with expected P fixation in the iron oxide-rich clay horizons (i.e., B_t layer). Based on the model output, rates of P leaching into the soil profile over 150-years of agriculture and afforestation could account for ~ 7–20 kg ha^{-1} P movement. Foroughi (2019) estimated extractable P (Mehlich-III P) in watersheds of the Calhoun CZO that have historical agricultural land to be 33 kg ha^{-1} (through a 2 m soil profile) greater than profiles in hillslopes with no agricultural history. This result suggests vertical P leaching over decades may account for most of the observed increase in subsoil extractable P. Soil extractable and total P could be enriched in prior agricultural land due to fertilization or manure application (MacDonald et al. 2012). Thus, part of the agricultural legacy of elevated extractable P can be leached through the soil profile, particularly during afforestation and the associated increase in soil infiltration. As noted earlier, soil infiltration increases during reforestation due to the recovery of soil macropores, increased soil organic matter, and better soil structure (Mapa 1995). Increases in infiltration with reforestation have been widely observed (Filoso et al. 2017).

Simulation under high rainfall further increased P leaching to the second soil horizon from 0.06 to 0.27 kg ha^{-1} year^{-1} under deciduous forest and agriculture-deciduous forest. The highest leaching of P was associated with agriculture, which increased from 0.036 to 0.33 kg ha^{-1} year^{-1} with a twofold increase in rainfall. Under agriculture abandonment (pine forest-agriculture) P leaching increased threefold due to high rainfall. Similarly, P leaching increased from 0.1 or 0.05 kg ha^{-1} year^{-1} to > 0.3 kg ha^{-1} year^{-1} under pine forest and mixed forest, respectively (Fig. 8). Incorporating high precipitation into model simulations for the various land-uses resulted in the content of P leaching to subsoil layers to increase five to ninefold largely due to an increasing volume of water infiltration. Previous work has similarly demonstrated how periods of saturated soil conditions under forest or agroforestry conditions can enhance P mobility by 50–70% relative to unsaturated soil conditions (Maranguit et al. 2017). Thus, leaching of P into subsoil layers over decades of land-use change in the Calhoun CZO may well have been enhanced during high rainfall years or specific high rainfall events (i.e., hurricanes). The novel observation of an increase in soil extractable P concentration through a 2 m clay-rich soil profile with an agriculture history is counter to perceptions of soil P immobility. The model simulations over a long-term trajectory of land-use change including high rainfall periods suggest the 33 kg-P ha^{-1} increase through 2 m of the soil profile could be accounted for by P concentrations and contents in vertical leaching.

Conclusion

Two centuries of land-use history in the Calhoun CZO has followed a trajectory of forest to agriculture to afforestation that has left a legacy of P enrichment and redistribution. In model outputs, stream water losses of P increased with decreasing forest proportion and increased inputs of P fertilizer during agriculture while during afforestation P stream water fluxes declined, all expected responses. Phosphorus leaching vertically through soils followed a different pattern. The highest P leaching rates to subsurface soil were observed under afforesting conditions when soil P was elevated, but so were surface soil infiltration rates. Modeled concentrations of solution inorganic P in leachate at the end of the afforestation trajectory were similar to soil solution concentrations we measured in 2016 to 2018 (0.48–0.55 and 0.2–0.6 μmol-P L^{-1} P at 15 cm and 60 cm, respectively). On the other hand, our measurements of soil total P contents that showed no difference between historically farmed and unfarmed watersheds could not be well-explained by P losses in the model even at 4.5 kg ha^{-1} $year^{-1}$ under agriculture with high rainfall. If fertilizer inputs were 7500 kg ha^{-1} over the long sweep of 150-years, P loss would account for < 1000 kg ha^{-1}. In contrast, subsurface soil increases in extractable P through 2 m of ~ 33 kg-P ha^{-1} were consistent with model leaching estimates over the agriculture to afforestation period of the trajectory. Vertical leaching fluxes of ~ 40 kg-P ha^{-1} could account for the entire soil profile increase.

This study revealed how historical land-use changes may have affected P movement from soil to stream and how increased rainfall has the potential to amplify the loss of P with runoff. Deforestation and cultivation of the watershed increased streamflow and P loss from soil to stream, particularly with agricultural P fertilizer. Higher magnitude rainfall had a positive effect on P movement that combined with land-use scenarios increased P content in streamflow. Phosphorus fluxes in stream water declined with afforestation after agricultural land abandonment. The estimated losses of P over this historical trajectory, however, suggested a lower historic P fertilization rate than presumed here. The model also highlighted that afforestation coincided with a shift from surface runoff and erosion to infiltration and vertical leaching of P at a magnitude consistent with currently observed extractable subsoil P increases. It will be difficult to improve estimates of historical fertilizer inputs. On the other hand, continuing to better reconcile retention of surface soil P from historic agriculture with observations of elevated extractable P at depth, possibly due to episodic vertical leaching should be possible. Our work highlights how P leaching though at least 2 m depth may occur in spite of presumed immobility.

Acknowledgements We acknowledge the leadership and guidance of Dr. Daniel D. Richter at the Calhoun CZO and the help of Will Cook, Zhine Wang, and Drs. Jill Qi, and Nahal Hoghooghi to improve this manuscript.

Funding This research was funded by the National Science Foundation (NSF) through the Geosciences Directorate's Division of Earth Sciences Critical Zone Observatory Program (EAR-1331846).

Declarations

Conflict of interest There are no known conflicts of interest associated with this publication and the authors declare that they have no known competing financial interests or personal relationships that could have appeared to influence the work reported in this paper.

References

Abbaspour KC (2012) SWAT-CUP-2012. SWAT Calibration and Uncertainty Analysis Programs—A User Manual. Swiss Federal Institute of Aquatic Science and Technology, Dübendorf, Switzerland

Abbaspour KC, Yang J, Maximov I, Siber R, Bogner K, Mieleitner J, Zobrist J, Srinivasan R (2007) Modelling hydrology and water quality in the pre-alpine/alpine Thur watershed using SWAT. J Hydrol 333:413–430. https://doi.org/10.1016/j.jhydrol.2006.09.014

Aguiar AdCF, Cândido CS, Carvalho CS, Monroe PHM, de Moura EG (2013) Organic matter fraction and pools of phosphorus as indicators of the impact of land use in the Amazonian periphery. Ecol Indicators 30:158–164. https://doi.org/10.1016/j.ecolind.2013.02.010

Akhtar MS, Richards BK, Medrano PA, DeGroot M, Steenhuis TS (2003) Dissolved phosphorus from undisturbed soil cores. Soil Sci Soc Am J 67:458–470. https://doi.org/10.2136/sssaj2003.4580

Alt F, Oelmann Y, Herold N, Schrumpf M, Wilcke W (2011) Phosphorus partitioning in grassland and forest soils of Germany as related to land-use type, management intensity, and land use–related pH. J Plant Nutr Soil Sci 174:195–209. https://doi.org/10.1002/jpln.201000142

Arabi M, Govindaraju RS, Hantush MM, Engel BA (2006) Role of watershed subdivision on modeling the effectiveness of best management practices with SWAT. J Am Water Resour Assoc 42:513–528. https://doi.org/10.1111/j.1752-1688.2006.tb03854.x

Arnold JG, Allen PM, Bernhardt G (1993) A comprehensive surface-groundwater flow model. J Hydrol 142:47–69. https://doi.org/10.1016/0022-1694(93)90004-S

Arnold JG, Srinivasan R, Muttiah RS, Williams JR (1998) Large area hydrologic modeling and assessment part I: model development. J Am Water Resour Assoc 34:73–89. https://doi.org/10.1111/j.1752-1688.1998.tb05961.x

Brender E (1952) From forest to farm to forest again. Am For 58:24–25

Brown AE, Zhang L, McMahon TA, Western AW, Vertessy RA (2005) A review of paired catchment studies for determining changes in water yield resulting from alterations in vegetation. J Hydrol 310:28–61. https://doi.org/10.1016/j.jhydrol.2004.12.010

Byers HL, Cabrera ML, Matthews MK, Franklin DH, Andrae JG, Radcliffe DE, McCann MA, Kuykendall HA, Hoveland CS, Calvert VH (2005) Phosphorus, sediment, and *Escherichia coli* loads in unfenced streams of the Georgia Piedmont, USA. J Environ Qual 34:2293–2300. https://doi.org/10.2134/jeq2004.0335

Carpenter SR, Caraco NF, Correll DL, Howarth RW, Sharpley AN, Smith VH (1998) Nonpoint pollution of surface waters with phosphorus and nitrogen. Ecol Appl 8:559–568. https://doi.org/10.1890/1051-0761(1998)008[0559:NPOSWW]2.0.CO;2

Chaubey I, Migliaccio K, Green C, Arnold J, Srinivasan R (2006) Phosphorus modeling in soil and water assessment tool (SWAT) model. Book modeling phosphorus in the environment. CRC Press

Compton JE, Boone RD (2000) Long-term impacts of agriculture on soil carbon and nitrogen in New England forests. Ecology 81:2314–2330. https://doi.org/10.1890/0012-9658(2000)081[2314:LTIOAO]2.0.CO;2

Cowell CM (1998) Historical change in vegetation and disturbance on the Georgia Piedmont. Am Midl Nat 140:78–90. https://doi.org/10.1674/0003-0031(1998)140[0078:HCIVAD]2.0.CO;2

Deng Q, McMahon DE, Xiang Y, Yu CL, Jackson RB, Hui D (2017) A global meta-analysis of soil phosphorus dynamics after afforestation. New Phytol 213:181–192. https://doi.org/10.1111/nph.14119

Dillon PJ, Kirchner W (1975) The effects of geology and land use on the export of phosphorus from watersheds. Water Res 9:135–148. https://doi.org/10.1016/0043-1354(75)90002-0

El-Khoury A, Seidou O, Lapen D, Que Z, Mohammadian M, Sunohara M, Bahram D (2015) Combined impacts of future climate and land use changes on discharge, nitrogen and phosphorus loads for a Canadian river basin. J Environ Manage 151:76–86. https://doi.org/10.1016/j.jenvman.2014.12.012

Elrashidi M, Mays M, Harder J, Schroeder D, Brakhage P, Peaslee S, Seybold C, Schaecher C (2005) Loss of phosphorus by runoff for agricultural watersheds. Soil Sci 170:543–558

Filoso S, Bezerra MO, Weiss KC, Palmer MA (2017) Impacts of forest restoration on water yield: a systematic review. PLoS ONE 12:e0183210. https://doi.org/10.1371/journal.pone.0183210

Foroughi M (2019) Soil Phosphorus biogeochemistry in the Critical Zone Observatory, South Carolina: effects of Land use, Topography, and Time. Dissertation, University of Georgia

Foster D, Swanson F, Aber J, Burke I, Brokaw N, Tilman D, Knapp A (2003) The importance of land-use legacies to ecology and conservation. Bioscience 53:77–88. https://doi.org/10.1641/0006-3568(2003)053[0077:TIOLUL]2.0.CO;2

Gassman PW, Reyes MR, Green CH, Arnold JG (2007) The soil and water assessment tool: historical development, applications, and future research directions. Trans ASABE 50:1211–1250. https://doi.org/10.13031/2013.23637

Goyette J-O, Bennett E, Maranger R (2018) Low buffering capacity and slow recovery of anthropogenic phosphorus pollution in watersheds. Nat Geosci. https://doi.org/10.1038/s41561-018-0238-x

Gray LC, Thompson EK (1933) History of agriculture in the southern United States to 1860. Nature. https://doi.org/10.1038/132838a0

Grieve IC (2001) Human impacts on soil properties and their implications for the sensitivity of soil systems in Scotland. Catena 42:361–374. https://doi.org/10.1016/S0341-8162(00)00147-8

Hall AR (1949) Terracing in the southern Piedmont. Agric Hist 23:96–109

Hart JF (1980) Land use change in a piedmont county. Ann Assoc Am Geogr 70:492–527

Hornbeck J, Adams M, Corbett E, Verry E, Lynch J (1993) Long-term impacts of forest treatments on water yield: a summary for northeastern USA. J Hydrol 150:323–344. https://doi.org/10.1016/0022-1694(93)90115-P

Huisman NL, Karthikeyan K (2012) Using radiometric tools to track sediment and phosphorus movement in an agricultural watershed. J Hydrol 450:219–229. https://doi.org/10.1016/j.jhydrol.2012.05.007

Hurtt GC, Frolking S, Fearon M, Moore B, Shevliakova E, Malyshev S, Pacala SW, Houghton R (2006) The underpinnings of land-use history: three centuries of global gridded land-use transitions, wood-harvest activity, and resulting secondary lands. Global Change Biol 12:1208–1229. https://doi.org/10.1111/j.1365-2486.2006.01150.x

Ireland HA, Sharpe CFS, Eargle D (1939) Principles of gully erosion in the Piedmont of South Carolina. U.S. Dept. of Agriculture. https://doi.org/10.22004/ag.econ.167374

Jiang S, Hua H, Jarvie HP, Liu X, Zhang Y, Sheng H, Liu X, Zhang L, Yuan Z (2018) Enhanced nitrogen and phosphorus flows in a mixed land use basin: drivers and consequences. J Clean Prod 181:416–425. https://doi.org/10.1016/j.jclepro.2018.02.005

Johnes P, Heathwaite AL (1997) Modelling the impact of land use change on water quality in agricultural catchments. Hydrol Process 11:269–286. https://doi.org/10.1002/(SICI)1099-1085(19970315)11:3<269::AID-HYP442>3.0.CO;2-K

Jones JA, Post DA (2004) Seasonal and successional streamflow response to forest cutting and regrowth in the northwest and eastern United States. Water Resour Res 40:1–19. https://doi.org/10.1029/2003WR002952

Leinweber P, Meissner R, Eckhardt KU, Seeger J (1999) Management effects on forms of phosphorus in soil and leaching losses. Eur J Soil Sci 50:413–424. https://doi.org/10.1046/j.1365-2389.1999.00249.x

Lindstrom M, Schumacher T, Blecha M (1994) Management considerations for returning CRP lands to crop production. J Soil Water Conserv 49:420–425

MacDonald GK, Bennett EM, Taranu ZE (2012) The influence of time, soil characteristics, and land-use history on soil phosphorus legacies: a global meta-analysis. Global Change Biol 18:1904–1917. https://doi.org/10.1111/j.1365-2486.2012.02653.x

Mallard JM (2017) CZO Dataset: Calhoun CZO - Precipitation (2014-2017), Retrieved 23 Jun 2019. http://criticalzone.org/calhoun/data/dataset/6421/

Mallard JM (2018) Calhoun CZO Stream Discharge/Runoff, HydroShare. https://www.hydroshareorg/resource/ad719c838a7b44e8bbacb33d2c4dd95f/

Mapa RB (1995) Effect of reforestation using Tectona grandis on infiltration and soil water retention. For Ecol Manage 77:119–125. https://doi.org/10.1016/0378-1127(95)03573-S

Maranguit D, Guillaume T, Kuzyakov Y (2017) Land-use change affects phosphorus fractions in highly weathered tropical soils. Catena 149:385–393. https://doi.org/10.1016/j.catena.2016.10.010

McLauchlan K (2006) The nature and longevity of agricultural impacts on soil carbon and nutrients: a review. Ecosystems 9:1364–1382. https://doi.org/10.1007/s10021-005-0135-1

Mehdi B, Ludwig R, Lehner B (2015) Evaluating the impacts of climate change and crop land use change on streamflow, nitrates and phosphorus: a modeling study in Bavaria. J Hydrol Reg Stud 4:60–90. https://doi.org/10.1016/j.ejrh.2015.04.009

Metz LJ (1958) The Calhoun Experimental Forest. https://www.fs.usda.gov/treesearch/pubs/927

Monteith JL (1965) Evaporation and environment. Symp Soc Exp Biol 19:205–234

Nash JE, Sutcliffe JV (1970) River flow forecasting through conceptual models part I—A discussion of principles J Hydrol 10:282–290. https://doi.org/10.1016/0022-1694(70)90255-6

Neitsch SL, Arnold JG, Kiniry JR, Williams JR (2011) Soil and water assessment tool theoretical documentation version 2009. Texas Water Resources Institute

Nielsen A, Trolle D, Søndergaard M, Lauridsen TL, Bjerring R, Olesen JE, Jeppesen E (2012) Watershed land use effects on lake water quality in Denmark. Ecol Appl 22:1187–1200. https://doi.org/10.1890/11-1831.1

USDA-NRCS (2004) Estimation of direct runoff from storm rainfall. National Engineering Handbook Hydrology, Chapter 10, Part 630

Osborne LL (1988) Empirical relationship between land use/-cover and stream water quality in an agricultural watershed. J Environ Manage 26:9–27

Parfitt R (1978) Anion adsorption by soils and soil materials. Adv Agron 30:1–50. https://doi.org/10.1016/S0065-2113(08)60702-6

Pettus L (1995) Surveying practices in early South Carolina. Backsights Magazine

Richter DD, Markewitz D (2001) Understanding soil change: soil sustainability over millennia, centuries, and decades. Cambridge University Press, Cambridge

Richter DD, Allen HL, Li J, Markewitz D, Raikes J (2006) Bioavailability of slowly cycling soil phosphorus: major restructuring of soil P fractions over four decades in an aggrading forest. Oecologia 150:259–271. https://doi.org/10.1007/s00442-006-0510-4

Rocha J, Roebeling P, Rial-Rivas ME (2015) Assessing the impacts of sustainable agricultural practices for water quality improvements in the Vouga catchment (Portugal) using the SWAT model. Sci Total Environ 536:48–58. https://doi.org/10.1016/j.scitotenv.2015.07.038

Ruffin E (1852) An essay on calcareous manures. JW Randolph

Schmidt J, Buol S, Kamprath E (1997) Soil phosphorus dynamics during 17 years of continuous cultivation: a method to estimate long-term P availability. Geoderma 78:59–70. https://doi.org/10.1016/S0016-7061(97)00011-6

Sharpley A (1985) Depth of surface soil-runoff interaction as affected by rainfall, soil slope, and management. Soil Sci Soc Am J 49:1010–1015. https://doi.org/10.2136/sssaj1985.03615995004900040044x

Sharpley AN, Smith S (1990) Phosphorus transport in agricultural runoff: the role of soil erosion. Paper presented at the Soil erosion on agricultural land. In: Proceedings of a workshop sponsored by the British Geomorphological Research Group, Coventry, UK, January 1989

Sharpley AN, Withers PJ (1994) The environmentally-sound management of agricultural phosphorus. Fertil Res 39:133–146. https://doi.org/10.1007/BF00750912

Sharpley A, Ahuja L, Menzel R (1981) The release of soil phosphorus to runoff in relation to the kinetics of desorption. J Environ Qual 10:386–391. https://doi.org/10.2134/jeq1981.00472425001000030029x

Sharpley A, Daniel T, Sims J, Pote D (1996) Determining environmentally sound soil phosphorus levels. J Soil Water Conserv 51:160–166

Sheridan RC (1979) Chemical fertilizers in southern agriculture. Agric Hist 53:308–318

Stoy PC, Katul GG, Siqueira MB, Juang JY, Novick KA, McCarthy HR, Christopher Oishi A, Uebelherr JM, Kim HS, Oren R (2006) Separating the effects of climate and vegetation on evapotranspiration along a successional chronosequence in the southeastern US. Global Change Biol 12:2115–2135. https://doi.org/10.1111/j.1365-2486.2006.01244.x

Swank WT, Vose J, Elliott K (2001) Long-term hydrologic and water quality responses following commercial clearcutting of mixed hardwoods on a southern Appalachian catchment. For Ecol Manage 143:163–178

Taylor RH (1953) Fertilizers and farming in the southeast, 1840–1950: Part I: 1840–1900. N C Hist Rev 30:305–328

Tong ST, Sun Y, Ranatunga T, He J, Yang YJ (2012) Predicting plausible impacts of sets of climate and land use change scenarios on water resources. Appl Geogr 32:477–489. https://doi.org/10.1016/j.apgeog.2011.06.014

Trimble SW (2008) Man-induced soil erosion on the Southern Piedmont, 1700–1970, 2nd edn. Soil and Water Conservation Society, Ankeny

Trimble SW, Weirich FH, Hoag BL (1987) Reforestation and the reduction of water yield on the Southern Piedmont since circa 1940. Water Resour Res 23:425–437. https://doi.org/10.1029/WR023i003p00425

Turner MG, Ruscher CL (1988) Changes in landscape patterns in Georgia, USA. Landscape Ecol 1:241–251. https://doi.org/10.1007/BF00157696

Ullrich A, Volk M (2009) Application of the Soil and Water Assessment Tool (SWAT) to predict the impact of alternative management practices on water quality and quantity. Agric Water Manage 96:1207–1217. https://doi.org/10.1016/j.agwat.2009.03.010

Veldkamp A, Verburg PH (2004) Modelling land use change and environmental impact. J Environ Manage. https://doi.org/10.1016/j.jenvman.2004.04.004

Vogt JT, Smith WB (2017) USDA Forest Inventory and Analysis Fiscal Year 2016 Business Report. https://www.fs.fed.us/sites/default/files/15817-usda-forest-service-fia-annual-report-508-update.pdf

Von Randow RCS, Rodriguez DA, Tomasella J, Aguiar APD, Kruijt B, Kabat P (2019) Response of the river discharge in the Tocantins River Basin, Brazil, to environmental changes and the associated effects on the energy potential.

Reg Environ Change 19:193–204. https://doi.org/10.1007/s10113-018-1396-5

Wang Q, Xiao Q, Liu C, Wang K, Ye M, Lei A, Song X, Kohata K (2012) Effect of reforestation on nitrogen and phosphorus dynamics in the catchment ecosystems of subtropical China: the example of the Hanjiang River basin. J Sci Food Agric 92:1119–1129. https://doi.org/10.1002/jsfa.4607

Wang X, Shang S, Yang W, Clary CR, Yang D (2010) Simulation of land use–soil interactive effects on water and sediment yields at watershed scale. Ecol Eng 36:328–344. https://doi.org/10.1016/j.ecoleng.2008.11.011

Wear DN, Greis JG (2013) The southern forest futures project: technical report. Gen Tech Rep SRS-GTR-178 Asheville, NC: USDA-Forest Service. Southern Research Station 178:1–542. https://doi.org/10.2737/SRS-GTR-178

Williams M (1992) Americans and their forests: a historical geography. Cambridge University Press

Wilson CO, Weng Q (2011) Simulating the impacts of future land use and climate changes on surface water quality in the Des Plaines River watershed, Chicago Metropolitan Statistical Area, Illinois. Sci Total Environ 409:4387–4405. https://doi.org/10.1016/j.scitotenv.2011.07.001

Zimmerman A, Johnson R, Hoover TS, Hilton J, Heinemann PH, Buckmaster D (2006) Comparison of personality types and learning styles of engineering students, agricultural systems management students, and faculty in an agricultural and biological engineering department. Trans ASABE 49:311–317. https://doi.org/10.13031/2013.20213